Self-Stabilizing Colonic Capsule Endoscopy: Pilot Study of Acute Canine Models

Dobromir Filip, Orly Yadid-Pecht, Christopher N. Andrews, and Martin P. Mintchev*

***Abstract*—Video capsule endoscopy (VCE) is a noninvasive method for examining the gastrointestinal tract which has been successful in small intestine studies. Recently, VCE has been attempted in the colon. However, the capsule often tumbles in the wider colonic lumen, resulting in missed regions. Self-stabilizing VCE is a novel method to visualize the colon without tumbling. The aim of the present study was to comparatively quantify the effect of stabilization of a commercially available nonmodified capsule endoscope (CE) MiroCam and its modified self-stabilizing version in acute canine experiments. Two customized MiroCam CEs were reduced in volume at the nonimaging back-end to allow the attachment of a self-expanding, biocompatible stabilizing device. Four mongrel dogs underwent laparotomy and exteriorization of a 15-cm segment of the proximal descending colon. A single CE, either self-stabilizing or nonmodified was inserted through an incision into the lumen of the colon followed by pharmacologically induced colonic peristalsis. The inserted capsule was propelled distally through the colon and expelled naturally through the anus. Novel signal processing method was developed to quantify the video stabilization based on camera tracking a predetermined target point (locale). The average locale trajectory, the average radius movement of the locale, and the maximum rate of change of the locale for sequential images were significantly lower for the stabilized capsules compared to the nonstabilized ones ($p < 0.05$). The feasibility of self-stabilized capsule endoscopy has been demonstrated in acute canine experiments.**

***Index Terms*—Colon, gastrointestinal tract, imaging, video capsule endoscopy.**

I. Introduction

COLON cancer is the most common gastrointestinal (GI) malignancy and the second leading cause of cancer deaths in the United States [1]. Of the many pre-neoplastic and neoplastic conditions in humans, nowhere is the ability to prevent disease as profound as it is in colon cancer [2]. Strategies for prevention have evolved over the past 15 years, now including the use of fecal occult blood test, fecal immunology tests, fecal DNA tests, colonoscopy, video capsule endoscopy (VCE), and computed tomographic (CT) colonography [3]. However, only colonoscopy, VCE, and CT colonography can visually detect small premalignant adenomatous colonic polyps, thus preventing the disease before it even starts.

The sensitivity of CT colonography for large adenomas appears to be high [4]. However, sensitivity for small, usually premalignant adenomas is very low [5]. This leaves colonoscopy and VCE as two possible screening methods to detect smaller premalignant polyps.

Traditional colonoscopy has been considered a routine, reliable, real-time, and quick method for assessing colonic abnormalities [6]–[8]. Moreover, it offers the ability to remove polyps during the procedure. Although classical colonoscopy can be considered safe, recent population-based studies have demonstrated that the rate of protection against colorectal cancer (CRC) that it offers is only 30%–50%. Tandem or "back-to-back" colonoscopies are procedures in which patients undergo two colonoscopic examinations in the same day [9], [10], and are considered more reliable than conventional colonoscopies [11]. Nevertheless, this technique has shown a pooled miss rate of polyps of any size as high as 22% [9].

Colonoscopy is an invasive procedure performed in a hospital setting, requires extensive and expensive logistic preparations, carries substantial risks of harming patients $(2\text{–}4/1000)$, is heavily operator-dependent, and requires postprocedural recovery [6]–[8]. During the procedure, the colon is shortened and crumpled in the process of inserting the colonoscope [12]. As a result, during withdrawal the most convoluted and crumpled parts can spring off the tip of the colonoscope at such speed that it is difficult to ensure a complete view [13]. The procedure requires conscious sedation or general anesthesia, constant medical supervision, and carries a risk of perforation of the colon [14].

Current flexible endoscopes cannot provide an image if the tissue is in contact with the tip of the endoscope because the so-called "red-out" occurs [15]. The majority of gastrointestinal endoscopies are performed with air inflation as required in order to improve image quality. Inflation, especially over-inflation, can sometimes cause imaging difficulties. Over-inflation can flatten polyps, making their edges harder to detect. In addition, over-distention of the bowel, with its consequent discomfort, is one of the issues making flexible colonoscopy an unpleasant and even dangerous examination [16].

Orally administered capsule endoscope (CE) is a simple, safe, noninvasive, and nonsedation requiring procedure. VCE is well accepted and tolerated by the patients and allows complete exploration of the small bowel [17]. Usually, it takes 24–48 h for a CE to pass through the entire GI tract as a result of its passive movement from mouth to anus [18]. In view of the fact that

Manuscript received May 02, 2011; revised July 18, 2011; accepted July 21, 2011. Date of publication July 29, 2011; date of current version December 02, 2011. This work was supported in part by Sandhill Scientific, USA and in part by Intromedic, Inc., Korea. *Asterisk indicates corresponding author.*

D. Filip and O. Yadid-Pecht are with the Department of Electrical and Computer Engineering, University of Calgary, Calgary, AB, T2N 1N4 Canada.

C. N. Andrews is with the Department of Medicine, Division of Gastroenterology, University of Calgary, Calgary, AB, T2N 1N4 Canada.

*M. P. Mintchev is with the Department of Electrical and Computer Engineering, University of Calgary, Calgary AB, T2N 1N4 Canada (e-mail: mintchev@enel.ucalgary.ca).

Digital Object Identifier 10.1109/TMI.2011.2163165

TABLE I
PILLCAM CCE: SENSITIVITY, SPECIFICITY, PPV AND NPV FOR ANY SIZE POLYPS AND SIGNIFICANT SIZE (>5 MM) POLYPS [24]

	Any size polyps	Polyps >5 mm
Sensitivity % (95% CI)	79 (61 - 90)	50 (19 - 81)
Specificity % (95% CI)	54 (35 - 70)	76 (63 - 86)
PPV %	63	20
NPV %	71	93
	X^2: p = 0.013	X^2: p > 0.05

the movement of these capsules is controlled by spontaneous gut peristalsis, the application of VCE is currently limited to small-lumen organs [19]. In larger-lumen organs, such as the stomach or the colon, the capsules tend to tumble, which leads to incorrect recognition of a given organ segment by the capsule imaging system, thus rendering the images unsuitable for diagnostic purposes and a miss rate in the colon exceeding 30% [20]. Temporary visual interferences and tumbling movements of the CEs include oblique-forward movement, oblique-reverse movement, perpendicular and rotational movements [21].

In addition, rapid colonic motility could result in incomplete imaging considering that most of the commercial CEs are designed to acquire images at a prefixed frame rate, usually two frames per second (FPS) [22]. Moreover, tumbling movement caused by peristalsis also limits the visual field, causes failure to catch significant lesions, or grossly distorts the perceived dimensions of polyps [23].

PillCam Colon capsule (Given Imaging, Yoqneam, Israel) is the only CE currently in use for colonic investigation. In the most recent study of 56 patients, colon capsule endoscopy (CCE) was followed by conventional colonoscopy (CSPY). Polyp detection rate (per patient) was 50% $(n = 28)$ for CSPY and 62% $(n = 35)$ for CCE. For relevant polyps (>5 mm) there was a correspondence in the detection rates of both methods $(p < 0.05)$. The mean sensitivity was 50% (95% confidence interval [CI], 19–81), the mean specificity was 76% (95% CI, 63–86), the positive predictive value (PPV) was 20% and the negative predictive value (NPV) was 93% [24]. Table I summarizes these results. Interestingly, the sensitivity for larger polyps is reduced, possibly due to the fact that the capsule cannot always present a panoramic view of the colonic tube with "the end of the colonic tunnel" at the center of the transmitted images. Instead, it often presents a view of the portion of the colonic wall closest to it, and if larger polyp encompasses the entire image its differential recognition becomes difficult if not impossible.

These results indicate the general problem of CCE tumbling during its transit in the colon and the need for its stabilization [23].

A. Aim of Study

The major goal of our study was to quantitatively compare the imaging capabilities of a conventional CE versus a custom-designed self-stabilized version of the same capsule endoscope during their separate transits in the colon in acute canine experiments.

II. METHODS

A. Standard Non-Modified Capsule Endoscopes

Two standard MiroCam (11×23 mm, 3.3 g; IntroMedic Co. Ltd., Seoul, Korea) capsule endoscopy systems were acquired for this experimental study. MiroCam capsules have an operating time of approximately 11 h, record data at 3 frames-per-second (fps), and deliver images at a resolution of 320×320 pixels. The 1.93-ml MiroCam device has automatic brightness control with six white light-emitting diodes (LEDs) which allows for optimized imaging and excellent image quality. In addition, the MiroCam provides high intraluminal details by using high-precision lens system that yields a 150° visual field. The complete system includes the MiroCam capsule, MiroView Workstation, MiroCam receiver, and a sensor array. MiroCam uses the human body as medium for transporting the images to the receiver [25]. After the procedure, the recorded data are transferred into the MiroView workstation for further image analysis.

B. Self-Stabilization Modification

Two customized MiroCam CEs were reduced in volume at the nonimaging back-end to a total of 1.72 ml to allow the reliable attachment of a custom-made, biocompatible stabilizing device.

Each self-stabilizing CE consisted of an outer casing and the modified MiroCam CE coupled to a stabilizing component. This stabilizing component was a thermally-treated, woven, biodegradable, liquid-permeable, flexible polyglactin 910 mesh (Vicryl, Ethicon Inc., Somerville, NJ) filled with superabsorbent polymer granules (Favor PAC, Evonik Industries, Stockhausen, Germany) [26].

Initially, the mesh was thermally processed to age it for a biodegradability of 2–3 days and to obtain oval shape (side length $= 2$ cm, radius $= 2$ cm) followed by cutting a slit (5 mm) through which the polymer (≈ 0.7 ml) was inserted into the oval-shaped mesh. Subsequently, the mesh was pulled over the end part of the CE through this opening, compactly attached to a specially designed lid using PDSII (USP 5-0) absorbable suture (Ethicon, Inc., Somerville, NJ), and covered with an outer casing (Torpac Inc., Fairfield, NJ). The outer casing was a hard-shell gelatin capsule which dissolved very rapidly (2–4 min) in water. This custom-made design was sized for animal testing, and with the design limitations in mind, a gelatin capsule of size #13 (1/8 oz. 3.2 ml) was chosen. The gelatin capsule provided an adequate space for the MiroCam CE containing both the electronics and the stabilizing component. Upon the degradation of the gelatin capsule, the permeable mesh containing the expandable polymer granules was exposed to colonic fluids, and swelled rapidly to the desired mushroom-like tail at the back of the imaging capsule.

The back-end of each capsule was ultra-fine threaded and a special cap which covered the fine thread was designed. This cap had a recessed groove, which was used to compactly attach the stabilizing component to the body of the imaging capsule

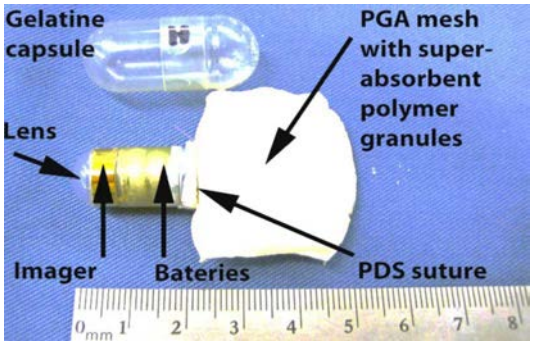

Fig. 1. Steps in assembling the self-stabilizing capsules. The expandable component made from permeable PGA mesh filled with superabsorbent polymer granules was attached to a reduced version of the MiroCam capsule containing only the batteries, the imager, and the lens. Subsequently, the entire implement was put in a gelatin capsule.

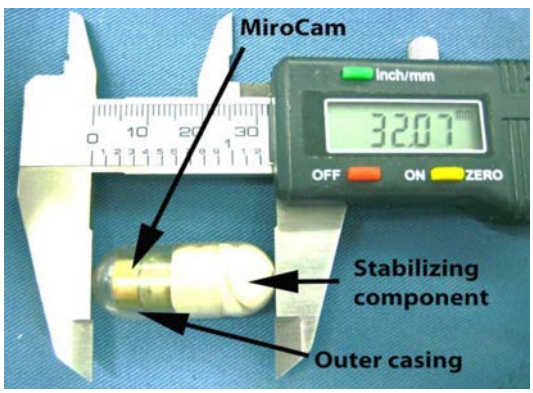

Fig. 2. Assembled self-stabilizing capsule endoscope. Length (in millimeters) is measured by a caliper.

using PDS II suture (Ethicon Inc., Somerville, NJ). The threaded cap was designed not only as a point of attachment of the stabilizing component, but also to provide a waterproof barrier for the back-end of the capsule. Aluminum was chosen as cap material because of its excellent combination of high wear resistance, low surface friction, high strength and great rigidity. Ultra-thin polytetrafluoroethylene (PTFE) film sealed the exposed threads before the cap was screwed into place.

The steps undertaken to assemble the capsules are outlined in Fig. 1. The two fully assembled self-stabilizing capsules (Fig. 2) were 33–35 mm in length in order to provide a meaningful comparison to Given Imaging PillCam Colon CE, which is 32 mm long [27].

A moisture-sensitive switch was placed on the surface of the self-stabilizing CEs, which activated the electronics inside the capsules after the outer casing dissolved, turning on the devices when in contact with colonic liquids.

In this design, the emphasis was on demonstrating stabilization and the testing assumed that the outer casing has reached the targeted organ. Thus, we used plain gelatin cover for the capsule. In a final design, a colon targeting film cover can be utilized such as the recently proposed coating prepared by mixing Eurylon VII [high amylose maize starch (Roquette, Lestrem, France)] aqueous dispersion and Eudragit S ethanolic solution (Evonik, Darmstadt, Germany) (ratio 3:7 solids) [28].

C. Details on the Design of the Stabilizing Component

The expandable material forming the stabilizing component should be able to deform under pressure but regain its original shape when the pressure is removed. The imperative requirements to the expandable component for providing maximal safety to patients are: 1) permeability to fluids and gases; 2) compliance characteristics mimicking soft stool; and 3) biodegradability in 2–3 days to avoid any possible obstruction in the gut. The expanded implement should also maintain its consistency and not change state under the influence of water, colonic fluids or pressure. The faster the expansion, the faster the imaging capsule would be stabilized in the colon, allowing quality imaging of the organ once the capsule enters the cecum. Thus, overall expansion time should be very short ($<$1 min). The materials that had the desired properties were categorized according to the preferred mechanism of expansion, osmosis (release of potential energy). Osmosis has proven to be effective in several medical applications such as stents that help relieve pathological obstruction of tubular structures in vascular, urologic and GI systems, as well as in self-expanding prostheses [29]. The availability of stent structures that can resist the peristaltic motion in the colon without them moving is indicative that osmosis should be the preferred mechanism for the proposed apparatus [30]. The expandable material used in this design was salt granules of hydrophyllic, nontoxic, crosslinked polyacrylate polymer. These granules can absorb several hundred times their weight in water, but cannot dissolve because of their 3-D polymeric network structure and only the formation of a gel takes place [31]. The use of this super-absorbent polymer as an expandable material for the device can be justified by its ability to be biocompatible, to swell extensively, to swell in a relatively short period of time, to exert a reasonable swelling pressure on the walls of the lumen, and to withstand the pressure in the colon by remaining attached to the imaging component while keeping its consistency. Moreover, when the superabsorbent polymer molecules are placed in water, hydrogen bonding with the surrounding liquids causes the molecules to unfold and to straighten out. When the molecules straighten out, they increase the viscosity of the surrounding liquid. This is very important during the CE transit in the colon since it allows for a very smooth movement of the capsule. The selected superabsorbent polymer provides high fluid retention even under pressure.

An important feature of the expandable component is also the requirement for sufficient flexibility to bend when passing through sharp colonic turns such as the hepatic and splenic flexures, similarly to the way formed stool does [32]. This bending capability should be uniform up to the base of the expandable component that is attached to the rigid, but relatively small imaging component.

Due to the geometry of the self-stabilizing CE and the pressure applied in the colon, there is a higher risk of the stabilizing and the imaging components disassociating from each other. Thus, the attachment point on the cap has been designed to maintain a strong connection between the CE and the stabilizing component utilizing PDS II suture. The attachment of the stabilizing component around the circumference of the sealable

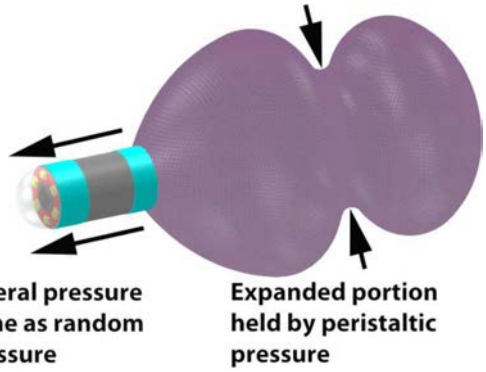

Fig. 3. Worst-case scenario for the stabilizing component where one end is held and the other is pulled by lateral and circumferential forces.

cap improves the strength of the connection, and prevents the two components from flexing. Additionally, this type of attachment normally preserves a common central axis between the two components, while ensuring the necessary flexibility when needed, for example when traversing through colonic flexures in a stool-like fashion.

The breaking strength of the stabilizing component should be greater than the maximum possible pressure in the colon if the worst-case scenario is considered. In this scenario, the peristaltic pressure holds one end of the stabilizing device fixed, while random pulling pressure is applied on the rest of the capsule. The random pressure is assumed to have a pulling effect, i.e., a lateral pressure of the same magnitude as the transversally applied random pressure. Fig. 3 shows the worst-case scenario from a point of view of separating the expandable component from the imager, when one end is held and the other is pulled laterally and circumferentially.

Colonic pressure activity is complex and usually ranges from 25 mmHg up to 400 mmHg [33]. A value of 400 mmHg (or 53 kPa) was used to calculate the worst-case scenario for the attachment between the CE imager and the expandable component. Thus, the bond between the imaging and the expanding components was designed to withstand maximal pressure of 53 kPa.

Previously, it was found that during colonoscopies externally produced intraluminal pressures above 140 mmHg (or 18.67 kPa) due to inflations can cause perforation of the colonic wall [34], [35]. Therefore, the average maximum swelling/expanding pressure exerted on the walls of the colon by the expandable component should not exceed that value. Thus, we designed the expandable component to create an average maximum swelling pressure of 16.67 kPa, or 124 mmHg. In addition, however, the permeability of the mesh to liquids and gases and the liquid-retaining capabilities of the superabsorbent polymer granules within it introduce a compliance feature of the expandable component similar to the compliance of an actual stool under colonic pressure. This creates an additional safety layer for the entire implement as it traverses through the colon and its average swelling pressure interacts with the colonic pressure. In the particular case of the FAVOR PAC superabsorbent polymer granules used in our study [36], the retention of liquid in the granules is 50 g/g at 1 kPa external pressure (7.5 mmHg), meaning that 1 g of dry granules holds 50 g of liquid at that pressure. Assuming linear relationship between applied pressure and water retention of gel beads in distilled water [37], an increase in pressure to 2 kPa (15 kPa) ensures retainment of 25 g of liquid for 1 g of dry polymer granules. In the proposed design, and under no external pressure, the maximal weight of the completely swollen expandable component in saline was 43 ± 6 g, while in the dry state it was 0.76 ± 0.5 g. Thus, at a colonic pressure of 53 kPa (the maximal possible in the organ), the weight of the expandable component can be expected to be reduced to approximately 0.81 g, i.e., almost to the level of the completely dry state. These dynamic shrinking-expanding characteristics of the expandable component under colonic pressure could be considered mimicking the actual swelling and shrinking of stool as it undergoes formation and molding in the colon [38]–[40]. In addition, it is interesting to point out that the permeability of the gauze to liquids can distort the linearity of the liquid retention characteristics of the superabsorbent polymer granules contained in it. For example, highly permeable gauze with wider pores would hardly influence it, while a gauze with smaller pores would help retaining more liquid in the swollen polymers under higher colonic pressures. This introduces another possible level of control of the dynamic properties of the expandable implement.

The antegrade propagating pressure is a component of the peristaltic pressure which is responsible for the distal movement of colonic content [41]. The mean peak amplitude of the antegrade propagating pressure waves in the colon is 41.8 ± 2.3 mmHg with a maximum of 169 mmHg [42]. This value should remain higher than the maximum swelling pressure of the expandable component, because otherwise severe constipation might result [43].

D. Self-Stabilizing CE Characteristics and Performance

An experimental setup was created to test the compliance of the fully expanded stabilizing component during the design optimization process. The quantitative measure of the compliance (elastance) $\mathcal{C}$ is often presented as the inverse of the elastic modulus, which is a measure of the increase in stress when strain is applied to a material as shown in (1) [44]–[46]

$$\boldsymbol{C} = \frac{\mathbf{1}}{\boldsymbol{E}} = \frac{\boldsymbol{\varepsilon}}{\boldsymbol{\sigma}} \tag{1}$$

where $\boldsymbol{E} =$ is elastic modulus of the expandable component, Pa; $\boldsymbol{\sigma} =$ is stress, Pa; $\boldsymbol{\varepsilon} =$ is strain, dimensionless.

The experimental setup (Fig. 4) consisted of the expandable stabilizing component (mesh and superabsorbent polymer), a transparent glass container ($5 \times 8 \times 9$ cm), liquid aqueous medium (saline or water), thin plastic plate (area of 1 inch^2), and a set of laboratory weights. Initially the container was filled with saline (height 1 cm). Once the expansion achieved its final swollen stage, the remaining liquid was removed from the glass container. Subsequently, the thin plastic plate was placed on the surface top part of the expanded stabilizing component. This plate was increasingly loaded with different laboratory weights, and the incremental force to cause a deformation to the expanded implement was recorded. As the external loading force was further increased, the vertical dimension started to

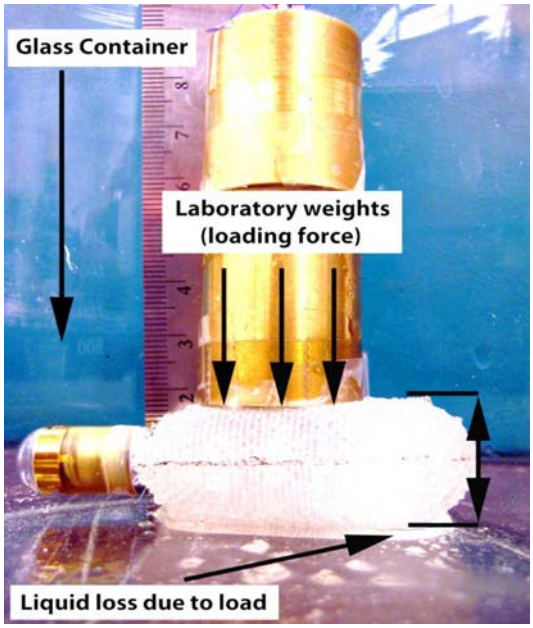

Fig. 4. Experimental setup for measuring maximum swelling pressure. From a certain laboratory weight on, the expanded stabilizing component started to decrease its volume. The contact surface area between the laboratory weight load and the expandable component was kept constant at 1 in^2.

decrease. The ratio between the reduced dimension resulting from a certain load and the initial dimension (without any load) gave a measure of the strain ε, which was determined to be linear for six consecutive loads ranging from 25 to 600 g. The stress σ was measured according to [47]

$$\boldsymbol{\sigma = \frac{F}{S} = \frac{mg}{S}} \tag{2}$$

where σ is is the stress in Pa; $\boldsymbol{m}$ is the mass of the loading weight in kg; g is the gravitational acceleration of 9.81 m/s^2; and $\boldsymbol{S}$ is the surface contact area between the weight and the expandable component in m^2 (which was kept constatnt at 1 inch^2 or 6.45×10^{-4} m^2). The strain was calculated using the following equation [48]:

$$\boldsymbol{\varepsilon = \frac{\Delta y}{y}} \tag{3}$$

where y is the original height of the expanded implement before loading with weights in m; and Δy is the change in height due to the loading force in m. The calculated strain and stress were utilized to determine the elastance C for each designed expandable component.

At a certain load the expanded implement started to decrease its volumetric size due to the fact that the polymer granules trapped within the mesh were not able to retain their liquid molecules contributing to the expanded state of each granule. This load was used to determine the maximum swelling pressure the expandable component can exert on the colonic walls before it would start collapsing. Subsequently, the tensile strength of the mesh was measured again by loading the expanded stabilizing component with gradually increasing laboratory weights until it completely collapsed. This measure ensured that the PGA mesh can be fully collapsed when under maximum peristaltic load without bursting.

The physical dimensions of the expandable stabilizing component were measured prior to and after expansion, and the expansion time was recorded. In addition, the volumetric size of the expandable component before and after the expansion was measured.

A total of 12 different designs of the expandable component were tested until the desired maximum swelling pressure was obtained. Once the desired design was achieved, the tests were repeated five times to ensure design repeatability. The compliance measure was utilized during this optimization process. The proposed compliance-based design methodology can be used to adjust the maximum swelling pressure to a desired lower value for increased safety precautions.

E. Acute Animal Testing

Four mongrel dogs (2M, 2F, 25.3 ± 4.5 kg) were vaccinated and dewormed as per the Canadian Veterinary Medical Association's recommended yearly protocol regime. Vaccines included Canine Distemper/Adenovirus, Type 2 Parvovirus/Bordetella/Rabies. Drontal Plus (Bayer HealthCare LLC, Shawnee Mission, KS) was used as oral dewormer. Each animal underwent physical examination by a board-certified veterinarian and was found to be in good condition. Colon preparation involved a 48-h liquid diet and the administration of phosphosoda enema in the morning before the surgery. At the end of the experiment the four animals were euthanized with an intravenous injection of Euthanyl, (480 mg/4.5 kg, Bimeda-MTC Animal Health Inc., Cambridge, ON, Canada). This research was approved by the Life and Environmental Sciences Animal Care Committee, University of Calgary, Calgary, AB, Canada.

Each of the animals underwent an induction with an intravenous injection of thiopental (Thiotal 15 mg/kg IV, Vetoquinol Canada, Lavaltrie, QC, Canada) and was subsequently maintained on inhalant isoflurane and oxygen (Halocarbon Laboratories, River Edge, NJ) with a vaporizer setting of 1%–3%. An array of eight receiving channels was attached to the external abdomen using standard ECG electrodes (CE, MiroCam; IntroMedic, Seoul, Korea) and connected to MiroCam receiver.

A laparotomy was followed by exteriorization of a 15 cm segment of the proximal descending colon while preserving intact the mesenteric innervations and blood supply. A 1-cm transverse full thickness incision was made in the colon 2 cm proximal to the beginning of the chosen colon segment.

A single CE, either self-stabilizing or nonmodified was inserted using forceps through the incision into the lumen of the colon. Subsequently, the incision was temporarily closed with 4-0 Dexon suture (Covidien, Mansfield, MA) and 200 ml saline was injected at the level of the capsule. The animal was then administered an intravenous injection of Neostigmine (0.04 mg/kg, APP Pharmaceuticals, Schaumburg, IL) which pharmacologically induced colonic peristalsis. The inserted capsule was propelled distally through the colon and expelled naturally through the anus as a result of the Neostigmine-induced colonic peristalsis. Upon the expulsion of the capsule through the anus, the video data which was collected by the attached MiroCam receiver were transferred to the MiroView Workstation for further image processing. After the clearance of Neostigmine from the circulation and ensuring that the animal recovered

fully from the previous procedure by monitoring its vital signs and particularly heart rate and blood pressure, another capsule was administered in a similar manner. This preserved the independent nature of the measurements for further statistical analysis. Ultimately, four such administrations per animal were sequentially performed, two with the nonstabilized and two with the stabilized capsules.

F. Digital Video Processing

A new image processing setup was developed to quantify the video stabilization with the help of a commercially-available camera tracking software package (Syntheyes, Andersson Technologies LLC, Malvern, PA). This setup included manual setting of the position of the specific feature (in our case, the lumen of the colon), feature size, search area and weight factor to track the feature, as well as a specific window size for the tracking field.

Feature tracking is used to monitor spatial and temporal changes in an object during a video sequence, including its presence, position, size, shape, etc. This is accomplished by solving the temporal correspondence problem, which essentially boils down to matching a predetermined target region or feature (also called locale) in successive frames of a sequence of images taken at closely-spaced time intervals, known as video frame sequence [49]. In brief, this algorithm tracks the motion of identifiable feature or features in an image stream. The method is able to match features of two images using spatial intensity gradient information with the help of a type of Newton–Raphson iterations [50]–[52].

Initially, the user places the 2-D track on a predetermined feature (locale), on the first frame and instructs the tracking program to follow the locale throughout the rest of the frame sequence. At the end of the automated tracking the program outputs data with X- and Y-fractional pixel coordinates of the tracked locale for each frame in the recorded video sequence.

The first step in quantifying the video sequences of the stabilized and unstabilized CEs was identifying the specific target region of interest, the locale. In the context of our task, locale is a target region (feature) located on the colonic axis which can be broadly defined as "the end of the colonic tunnel." It was already mentioned that the locale is a specific feature in the image that a feature tracking algorithm can lock onto and follow through multiple frames as the CE passes distally through the colon. If the CE imager would always point to this intraluminal locale it would not only be perfectly stabilized, but also would never miss any other areas during its slow transit distally through the colon. The initial locale was determined manually in the starting image of each video frame sequence before the tracking algorithm was applied to the rest of the video frames.

Since a specific intraluminal locale was tracked through video frames, a set of 2-D coordinates was created which was referred to as a tracker point (Fig. 5). These coordinates were then converted to video resolution $(\mathrm{Y} = 340, \mathrm{X} = 320)$ in a 2-D coordinate system with an origin at $(\mathrm{Y} = 170, \mathrm{X} = 160)$. If the locale left a given video frame, the latest recorded X-Y coordinates from the previous frame were assumed for each following image, until the locale appeared back on the latest video frame.

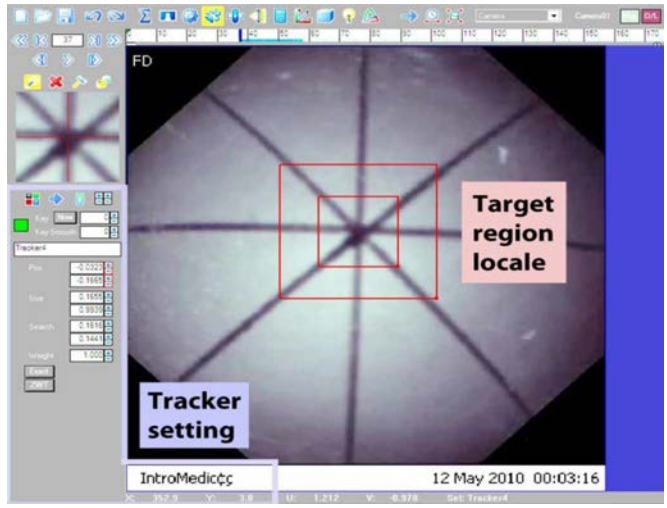

Fig. 5. Locale tracking in a simulated colon picture frame with a target region at the centroid.

This approach enabled to quantify data for both modalities (stabilized and unstabilized) without "outliers."

The next step involved data processing of the tracker Y-X coordinates in order to quantify the stabilization for both the stabilized and unstabilized CE. The image processing toolset included three different image processing techniques to quantify various aspects of the video sequences.

The first technique measured the average locale trajectory of the locale during the recorded video for both the stabilized and the unstabilized capsules. This approach calculated the distances between locale coordinates for two consecutive video frames. Subsequently, the obtained distances were put in an array for each capsule modality (stabilized or unstabilized). These distances were averaged to obtain the average locale trajectory per modality. In addition, the total locale trajectory per capsule modality (stabilized and unstabilized) was calculated by adding all distances between locale coordinates. This technique is a very simple indicator of the stabilization effect, since it measures the travelled distance of the locale. Still, it does not provide sufficient data to accurately quantify the stabilization effect.

In order to fill this void, a second technique called average radius movement was developed. This technique measured the distance of each coordinate of the locale from the center of the imager (170, 160) per frame for both CE modalities (stabilized and unstabilized). This was achieved by calculating minimum square distance between the origin of the coordinate system (170, 160) and the locale coordinates for each video frame in the sequence. After averaging the arrays containing these distances per capsule modality, a circle was synthesized which illustrated how much on the average the locale moved away from the central axis (centroid) of the capsule (average radius movement). Additionally, the standard deviation of each array was calculated to have a measure of volatility since the CE movement was expected to be random. This technique does provide sufficient data to numerically quantify the stabilized and the unstabilized CE videos. Unfortunately, it does not take into consideration the video frame rate dynamics in each of the two studied CE modalities (stabilized and nonstabilized).

Therefore, a third technique was developed, which measured the maximum rate of change for a given locale in consecutive video frames [pixel/sec] for each particular CE modality. Each video frame was converted into an image matrix 320×320 and the maximum change in pixels was measured by recording distances between the locales of two consecutive video frames. Subsequently, these distances were placed in an array per capsule modality, the two arrays were compared and the averages of both were calculated. This method is a clear indicator of the unvisualized areas and can also be utilized to estimate the average 3-D CE velocity. Then the average unvisualized area during CE transit can be quantified because the colon can be approximated by a cylinder in which the speed of transit of the imager is known.

Since all measurements in the three described quantitative techniques were collected in separate arrays for each capsule modality (stabilized and unstabilized) but the variances were generally not equal, they were statistically compared using the Welch's t-test and the significance level was chosen at $p < 0.05$ [53].

Additionally, a contour 3-D visualization has been developed using Matlab (MathWorks, Natick, MA) to illustrate the areas the locale occupied most frequently in the recorded videos. In this procedure, each video frame was converted into an image matrix (320×320). Initially this matrix was filled with zeroes. Pixel mask of the locale was projected onto this matrix for each video frame. This created a composite matrix with multiple pixel masks. If the masks overlapped the size of the resulting mask was doubled. In order to achieve a better visualization, the final matrix (image) with all the pixel masks from the entire video sequence was filtered by multiplying this matrix with a filter matrix for better visualization [54]. The resulting image was a bi-dimensional collection of pixels in rectangular coordinates, a contour 3-D graph which illustrated the most frequent areas the locale occupied in a video sequence for a given capsule modality (stabilized or unstabilized).

III. Results

A. Self-Stabilizing CE Characteristics and Performance

The volume of expandable component (polymer and mesh) was 0.76 ± 0.5 ml before expanding and 58 ± 7 ml after the expansion in water. The fully expanded volume in saline decreased to 43 ± 6 ml. Interestingly, the total volume of the self-stabilizing unit (the modified MiroCam capsule and the dry expandable stabilizing component) was in the range of 2.62 ml, which is still lower than the volume of 2.7 ml of Given's PillCam Colon capsule.

Prior to swelling each mesh had an oval shape of a 5.5 cm length and a diameter of 4 cm. The maximum swelling pressure that the expandable component exerted on the colonic walls before polymer granules started losing liquid and collapsing was determined to be 100 ± 18 mmHg. This value is well within the design constraints. Moreover, it is equivalent to 135.9 g/cm^2 and is also a measure of the consistency of the expandable component. Comparing this value to the mean consistency of stool in humans which has been reported as 300 g/cm^2 (measured using a very similar method to ours, [55]), it is quite clear that the consistency of our expandable component is quite lower. In the same line of thoughts, we considered it beneficial to compare the viscosity of the designed expandable component to the average viscosity of human stool. The dynamic viscosity of the swollen hydrogel that we utilized is in the range of 900–7000 centipoises (cPs) [56], while the dynamic mean soft stool viscosity in humans ranges between 50 000 to 100 000 cPs [57], indicating that the expandable component has lower viscosity (and therefore is closer to water) compared to soft human stool. The tensile strength of the mesh was 368 ± 22 mmHg, which was less than the maximal possible colonic pressure [32]. The expansion time was less than 1 min in water and less than 3 min in a saline solution. The saline solution contained heavy ions, which slowed down the osmosis process and lowered the volume of the fully swollen expandable component. The fully expanded capsule is shown in Fig. 6.

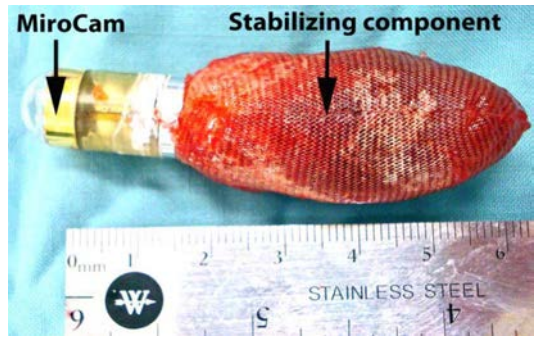

Fig. 6. Fully expanded self-stabilizing capsule endoscope. Due to its permeability, the mushroom-like tail swelled immediately after the degradation of the gelatin cover to provide stabilization to the imaging module.

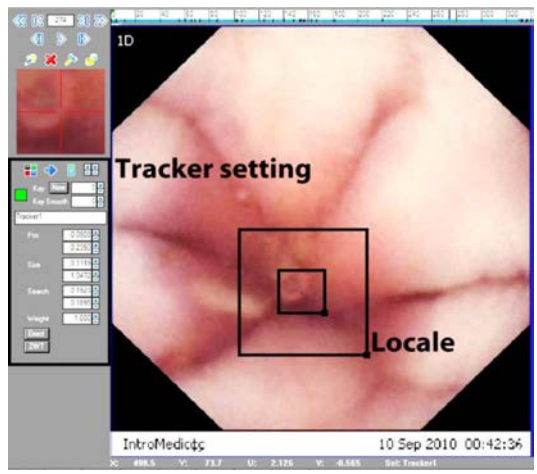

Fig. 7. Locale tracking in the colon with a target region at the centroid. Locale can be regarded in our case as "the end of the tunnel."

B. Acute Animal Testing

Totally, there were four video footages for each of the stabilized and the unstabilized cases, resulting in 1949 video frames for the former and in 1764 video frames for the latter. Fig. 7 shows a sample video frame (canine colon) from the tracking procedure in the Syntheyes camera tracker.

The average locale trajectory for the stabilized capsule was statistically significantly lower at 3.3 ± 4.8 pixels versus $17.2 \pm$

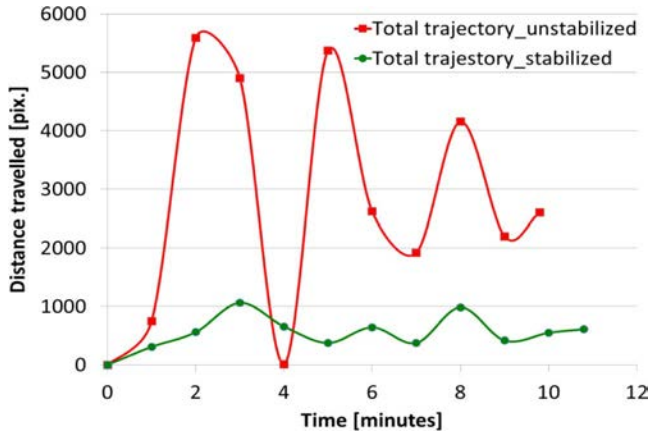

Fig. 8. Total locale trajectories per minute for the unstabilized (red) and stabilized (green) capsules.

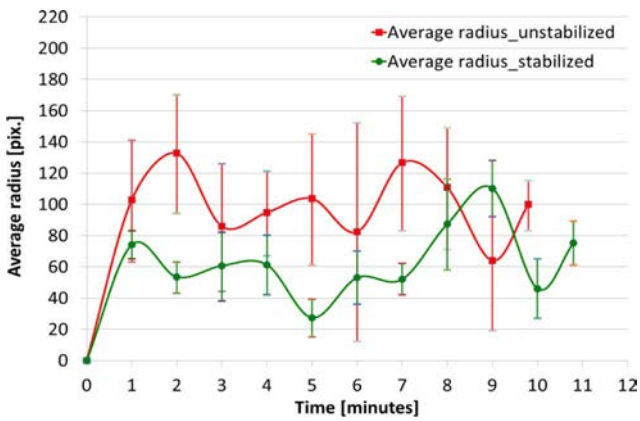

Fig. 9. Average radius movement per minute and its standard deviation for the unstabilized CEs (red) versus the stabilized capsules (green).

36.2 pixels for the nonstabilized ($p < 0.05$). The gross total local trajectory (obtained for the entire duration of all videos per modality) for the stabilized capsules was 4066 pixels versus 30 434 pixels for the unstabilized capsules. Fig. 8 illustrates graphically the obtained total locale trajectories in time intervals of 1 min for both capsule modalities (unstabilized and stabilized, respectively).

The average radius movement of the CE relative to the centroid of the colon was 63.5 ± 27.6 pixels for the stabilized capsule and statistically significantly higher at 100.4 ± 46.7 pixels for the unstabilized ($p < 0.05$). Fig. 9 represents graphically these differences per minute.

The maximum rate of change for sequential images was measured to be 43.7 ± 12 pixels/s for the stabilized case, while for the unstabilized it was statistically significantly higher at 445 ± 71.2 pixels/s ($p < 0.05$). Fig. 10 illustrates these differences.

In addition, the stabilized capsule showed significantly greater average improvement in the automated tracking of its recorded video versus the unstabilized capsule. The maximum rate of change was very high for the unstabilized CE and the automated tracker was not always able to continuously track the locale in consecutive video frames, resulting in assigning maximal coordinate values. Results for average locale trajectory, the average radius movement, and the maximum rate of

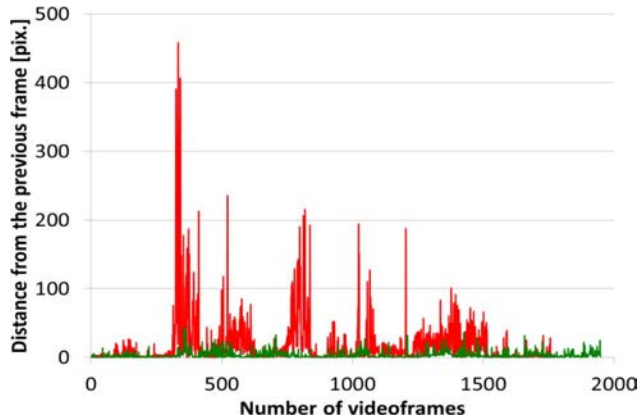

Fig. 10. Distances between the locales in successive video frames for the unstabilized (red) and the stabilized (green) capsules.

TABLE II
COMPARISON BETWEEN STABILIZED VERSUS UNSTABILIZED CE RESULTS

	Unstabilized CE	Self-Stabilizing CE
Average locale trajectory	17.2 ± 36.2	3.3± 4.8
Average radius	100.4±46.7	63.5±27.6
Maximum rate of change	445±71.2	43.7±12

change for the unstabilized and the stabilized CEs are shown in Table II.

Contour 3-D visualization is illustrated on Fig. 11 (stabilized capsule) and Fig. 12 (unstabilized capsule) to show the areas the respective locales occupied most frequently in the recorded videos. It is evident that during rapid capsule repositioning (e.g., during rapid peristaltic activity) the stabilized capsule reacted quickly by stabilizing itself towards the centroid of the lumen. This can be seen by comparing the positions of the maximum peaks (locale points) for both modalities (self-stabilizing and unstabilized) and their peak heights. The peaks were clustered around the centroid of the video frame for the stabilized CE, whereas for the unstabilized these peaks were widely spread. In addition, it can be observed that the locale had entirely disappeared from the video frames when the unstabilized capsule tumbled.

At no time in this study did the self-stabilizing capsule tumble within the colon to a point of the locale leaving the video frame. The simple reason for this was that both the combined length of the capsule and the stabilization mechanism exceeded the diameter of the lumen. Because the connection between the two was flexible, the completed assembly was unable to deform permanently, and the scenario in which the self-stabilizing CE could closely facing the colonic wall became a geometric impossibility with the fully expanded stabilizing component.

IV. DISCUSSION

In the quest for reliable colon cancer testing, colonoscopy has been considered the contemporary test of choice [58]. However, annual demand for colonoscopies in the United States ranges

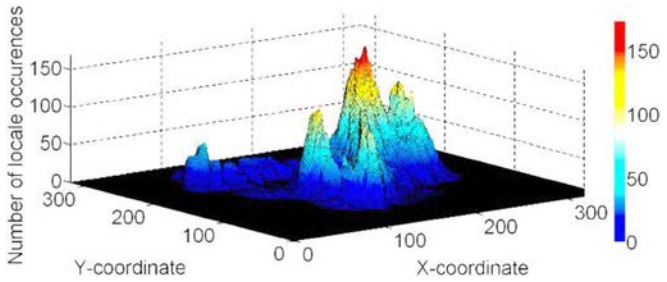

Fig. 11. Contour 3-D visualization for the self-stabilizing CE. The distribution of locales was concentrated in the central area of the video frames, with only one separate locale area at coordinates (250, 50), which, however, was still well within the area of the video frames.

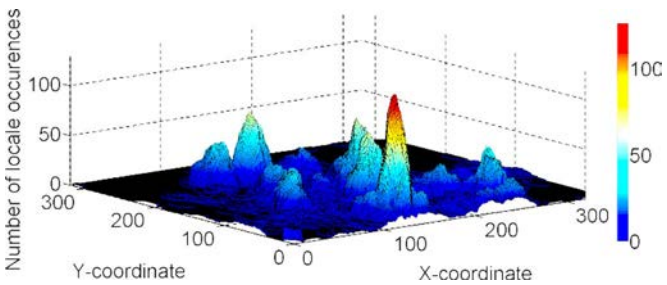

Fig. 12. Contour 3-D visualization for the unstabilized CE. The locales were far more distributed and some of them were even outside the area of the video frames.

from 2.21 to 7.96 million. As early as in 2004, an estimate was made that in order to provide colonoscopic cancer screening for every single American turning 65, the number of gastroenterologists performing the test nationwide would have to increase by at least 1360. If these tests are to be repeated every 10 years on any adult American, 32 700 more gastroenterologists will be needed [58]. This statistics does not even include the associated staff organizing, assisting and administering the test, nor the facilities needed for the testing. Obviously, a cheap, readily available, noninvasive cancer screening test that can be administered annually to the entire adult population would be of great benefit for controlling colon cancer nationwide.

VCE offers such noninvasive alternative for colon cancer screening and recently vigorous attempts have been made to adopt this technique [60]–[62]. Unfortunately, current capsule endoscopes experience tumbling and tossing problems in wider lumen organs such as the stomach or the colon [63], which diminishes their reliability.

In the present study, we offered a novel self-stabilizing design which greatly improved colonic CE imaging capabilities in acute canine models. We believe that the simplicity, the noninvasiveness, and the safety of this approach will greatly increase the scope and the perimeter of colon cancer screening prior to any symptoms appearing. The cost of the stabilizing-component is quite low and its design is pretty straightforward, with no adverse impact on safety and a minimal cost increment.

The proposed self-stabilizing solution offered no CE tumbling and tossing while traversing the canine colon. In addition, it was found to be safe and reliable. Although the reported results are very encouraging, further tests are needed to investigate the performance of the self-stabilizing VCE in humans, particularly with respect to 1) timed launching in the cecum; 2) safety if launched in the small intestine or in the stomach; 3) efficacy and safety, particularly with regards to the ability of the device to monitor its passages through sharp colonic flexures when traversing the entire colon, and not in the left colon only.

In order to address the timing issue, we offered as an idea a colon-targeting cover based on recently proposed coating [28], but did not actually test it. In the present design, safety was addressed by 1) designing the expandable component to exert a safe maximum swelling pressure on the colonic wall; 2) comparing the consistency and the dynamic viscosity of the designed expandable component to the ones of soft human stool; 3) making the mesh of the expandable component permeable and biodegradable; 4) quantifying the compliance of the expandable component so that an easy redesign can be performed if need be; and 5) incorporating small size swellable granules into the porous mesh, which not only can be naturally expelled through the colon even if they are fully expanded, but also are in contact with the colon through the pores of the mesh, thus determining the dynamic viscosity of the entire expandable component.

Further optimization of the expandable component can be performed, perhaps in the directions of increasing its consistency and its dynamic viscosity in order to achieve better stabilization results. However, particular attention should be paid these increased values not to exceed the average ones for soft human stool in order to avoid colonic transit problems and potential obstruction. In addition, an electronic safety mechanism can be incorporated into the capsule to separate the expandable component from the imaging part of the capsule. We have already designed such mechanism in the framework of a custom-designed self-stabilizing CE, and preliminary laboratory testing provided very encouraging results without putting any significant space demands [64].

Although the efficacy of the device in these canine tests appeared high, only actual human testing would be able to indicate whether a diagnostically meaningful, stabilized, and reliable human colon imaging can be achieved utilizing the proposed approach.

Finally, the scope of view of the self-stabilizing capsule can be enhanced by including wider-angle lens to examine better convoluted areas in the human colon [65], [66], or by changing the position of the imager from front to semilateral or lateral [67]–[69]. We expect that such modifications can only improve device performance, but the stabilizing effect would be achieved regardless.

V. Conclusion

The feasibility of self-stabilized capsule endoscopy has been demonstrated in acute canine experiments. New self-stabilized capsule design was described and was quantitatively compared to a regular, unstabilized CE. In comparison with the conventional MiroCam, the proposed self-stabilizing CE delivered a significant improvement in canine colonic imaging. The proposed device could be used for colorectal cancer screening of large-lumen organs and has the potential to greatly improve GI imaging quality. Since it mimics stool, it is permeable to liquids

and gases, and is short-term biodegradable, it is also safe and reliable. Further larger-scale clinical trials in humans are needed to confirm and elucidate further the findings of this pilot study.

REFERENCES

[1] A. Jemal *et al.*, "Cancer statistics," *CA Cancer J. Clin.*, vol. 60, pp. 277–300, 2010.

[2] V. W. Yang, J. Lewis, T. C. Wang, and A. K. Rustgi, "Colon cancer: An update and future directions," *Gastroenterology*, vol. 138, no. 6, pp. 2027–2028, 2010.

[3] A. V. Weizman and G. C. Nguyen, "Colon cancer screening in 2010: An update," *Minerva Gastroenterologica e Dietologica*, vol. 56, no. 2, pp. 181–188, 2010.

[4] C. Johnson *et al.*, "Accuracy of CT colonography for detection of large adenomas and cancers," *N. Eng. J. Med.*, vol. 359, pp. 1207–1217, 2008.

[5] W. Atkin, "Options for screening for colorectal cancer," *Scand. J. Gastroenterol.*, vol. 237, pp. 13–16, 2003, suppl.

[6] D. S. Weinberg, "Colonoscopy: What does it take to get it "Right"?," *Ann. Internal Med.*, vol. 154, no. 1, pp. 68–69, 2011.

[7] E. P. Whitlock *et al.*, *Screening for Colorectal Cancer: An Updated Systematic Review*. Rockville, MD: Agency Healthcare Res. Quality, 2008.

[8] G. Minoli *et al.*, "Quality assurance and colonoscopy," *Endoscopy*, vol. 31, no. 7, pp. 522–527, 1999.

[9] J. C. van Rijn, J. B. Reitsma, J. Stoker, P. M. Bossuyt, S. J. van Deventer, and E. Dekker, "Polyp miss rate determined by tandem colonoscopy: A systematic review," *Am J. Gastroenterol.*, vol. 101, no. 2, pp. 343–350, 2006.

[10] L. J. Hixson, M. B. Fennerty, R. E. Sampliner, and H. S. Garewal, "Prospective blinded trial of the colonoscopic miss-rate of large colorectal polyps," *J. Gastrointest. Endosc.*, vol. 37, no. 2, pp. 125–127, 1991.

[11] D. K. Rex, C. S. Cutler, G. T. Lemmel, E. Y. Rahmani, D. W. Clark, and D. J. Helper, "Colonoscopic miss rates of adenomas determined by back-to-back colonoscopies," *Gastroenterology*, vol. 112, no. 1, pp. 24–28, 1997.

[12] S. Thomas-Gibson and C. B. Williams, "Colonoscopy training-new approaches, old problems," *Gastrointest. Endosc. Clin. N. Am.*, vol. 15, no. 4, pp. 813–827, 2005.

[13] P. B. Cotton and C. H. B. Williams, "Colonoscopy and flexible sigmoidoscopy," in *Practical Gastrointestinal Endoscopy: The Fundamentals*, C. H. B. Williams, Ed., 6th ed. Oxford, U.K.: Wiley-Blackwell, 2008, pp. 164–165.

[14] D. K. Rex *et al.*, "Quality indicators for colonoscopy," *Am. J. Gastroenterol.*, vol. 101, no. 4, pp. 873–885, 2006.

[15] J. D. Waye, D. K. Rex, and C. B. Williams, "Insertion technique," in *Colonoscopy: Principles and Practice*, C. B. Williams, Ed., 2nd ed. Oxford, U.K.: Wiley Blackwell, 2003, pp. 539–543.

[16] P. Swain, "At a watershed? Technical developments in wireless capsule endoscopy," *J. Digestive Diseases*, vol. 11, no. 5, pp. 259–265, 2010.

[17] M. Munoz-Navas, "Capsule endoscopy," *World J. Gastroenterol.*, vol. 15, no. 13, pp. 1584–1586, 2009.

[18] W. El-Matary, "Wireless capsule endoscopy: Indications, limitations, and future challenges," *J. Pediatr. Gastroenterol. Nutr.*, vol. 46, no. 1, pp. 4–12, 2008.

[19] "Capsule endoscopy of the colon," *J. Gastrointest. Endosc.*, vol. 68, no. 4, pp. 621–623, 2008.

[20] R. Eliakim *et al.*, "Evaluation of the PillCam Colon capsule in the detection of colonic pathology: Results of the first multicenter, prospective, comparative study," *J. Endoscopy*, vol. 38, no. 10, pp. 963–970, 2006.

[21] H. M. Kim, Y. J. Kim, H. J. Kim, S. Park, J. Y. Park, S. K. Shin, J. H. Cheon, S. K. Lee, Y. C. Lee, S. W. Park, S. Bang, and S. Y. Song, "A pilot study of sequential capsule endoscopy using Mirocam and Pillcam SB devices with different transmission technologies," *J. Gut. Liver*, vol. 4, no. 2, pp. 192–200, 2010.

[22] D. Lieberman, "Progress and challenges in colorectal cancer screening and surveillance," *Gastroenterology*, vol. 138, no. 6, pp. 2115–2126, 2010.

[23] K. N. C. Hin, O. Yadid-Pecht, and M. Mintchev, "e-Stool: Self-stabilizng capsule for colonic imaging," in *Proc. 20th Int. Symp. Neurogastroenterol. Motility*, Jul. 3–6, 2005, pp. 86–90.

[24] J. B. Pilz, S. Portmann, P. Shajan, Ch. Beglinger, and L. Degen, "Colon capsule endoscopy compared to conventional colonoscopy under routine screening conditions," *J. BMC Gastroenterol.*, vol. 10, no. 66, 2010.

[25] S. Bang, J. Y. Park, S. Jeong, Y. H. Kim, H. B. Shim, T. S. Kim, D. H. Lee, and Y. Song, "First clinical trial of the "MiRo" capsule endoscope by using a novel transmission technology: Electric-field propagation," *J. Gastrointest. Endosc.*, vol. 69, no. 2, pp. 253–259, 2009.

[26] D. Filip, O. Yadid-Pecht, and M. P. Mintchev, "Progress in self-stabilizing capsules for imaging of the large intestine," in *Proc. 17th IEEE Int. Conf. Electron., Circuits Syst.*, Dec. 2010, pp. 231–234.

[27] A. Sieg, K. Friedrich, and U. Sieg, "Is PillCam COLON capsule endoscopy ready for colorectal cancer screening? A prospective feasibility study in a community gastroenterology practice," *Am. J. Gastroenterol.*, vol. 104, no. 4, pp. 848–854, 2009.

[28] V. C. Ibekwe, M. K. Khela, D. F. Evans, and A. W. Basit, "A new concept in colonic drug targeting: A combined pH-responsive and bacterially-triggered drug delivery technology," *Aliment Pharmacol. Ther.*, vol. 28, no. 7, pp. 911–916, 2008.

[29] A. Lauto, M. Ohebshalom, M. Esposito, J. Mingin, P. S. Li, D. Felsen, M. Goldstein, and D. P. Poppas, "Self-expandable chitosan stents: Design and preparation," *J. Biomaterials*, vol. 22, no. 13, pp. 1869–1874, 2001.

[30] E. Andersen and P. Ernst, "Medical stents for body lumens exhibiting peristaltic motion," U.S. Patent 6 505 654, Jan. 14, 2003.

[31] J. Haselbach, S. Hey, and T. Berner, "Short-term oral toxicity study of FAVOR PAC in rats," *J. Regulatory Toxicol. Pharmacol.*, vol. 32, no. 3, pp. 310–316, 2000.

[32] S. Nakaji, S. Fukuda, S. Iwane, H. Murakami, K. Tamura, A. Munakata, and K. Sugawara, "New method for the determination of fecal consistency and its optimal value in the general population," *J. Gastroenterol. Hepatol.*, vol. 17, no. 12, pp. 1278–1282, 2002.

[33] S. S. Rao, P. Sadeghi, J. Beaty, R. Kavlock, and K. Ackerson, "Ambulatory 24-h colonic manometry in healthy humans," *Am. J. Physiol. Gastrointest. Liver Physiol.*, vol. 280, no. 4, pp. 629–639, 2001.

[34] R. A. Kozarek and R. A. Sanowski, "Use of pressure release valve to prevent colonic injury during colonoscopy," *Gastrointest. Endosc.*, vol. 26, no. 4, pp. 139–142, 1980.

[35] B. G. Wolff, J. H. Pemberton, and S. D. Wexner, "Physiologic testing," in *The ASCRS Textbook of Colon and Rectal Surgery*, L. E. Smith and G. J. Blatchford, Eds., 1st ed. New York: Springer, 2007, pp. 45–46.

[36] *FAVOR-PAC DATA-Superabsorbent polymer for packaging applications*, , Feb. 23, 2011 [Online]. Available: http://www.stockhausen-inc.com/Products/Absorbent/favor-pac_data.htm

[37] M. Liu and T. Guo, "Preparation and swelling properties of crosslinked sodium polyacrylate," *J. Appl. Poly. Sci.*, vol. 82, no. 6, pp. 1515–1520, 2001.

[38] J. Hammer and S. F. Phillips, "Fluid loading of the human colon: Effects on segmental transit and stool composition," *Gastroenterology*, vol. 105, no. 4, pp. 988–998, 1993.

[39] L. P. Degen and S. F. Phillips, "How well does stool form reflect colonic transit?," *Gut*, vol. 39, no. 1, pp. 109–113, 1996.

[40] S. Nakaji, S. Fukuda, S. Iwane, H. Murakami, K. Tamura, A. Munakata, and K. Sugawara, "New method for the determination of fecal consistency and its optimal value in the general population," *J. Gastroenterol. Hepatol.*, vol. 17, no. 12, pp. 1278–1282, 2002.

[41] P. G. Dinning, M. M. Szczesniak, and I. J. Cook, "Proximal colonic propagating pressure waves sequences and their relationship with movements of content in the proximal human colon," *Neurograstroenterol. Mot.*, vol. 20, no. 5, pp. 512–520, 2008.

[42] I. J. Cook, Y. Furukawa, V. Panagopoulos, P. J. Collins, and J. Dent, "Relationships between spatial patterns of colonic pressure and individual movements of content," *Am. J. Physiol. Gastrointest. Liver Physiol.*, vol. 278, no. 2, pp. G329–G341, 2000.

[43] M. E. Pezim, J. H. Pemberton, K. E. Levin, W. J. Litchy, and S. F. Phillips, "Parameters of anorectal and colonic motility in health and in severe constipation," *Dis. Colon. Rectum.*, vol. 36, no. 5, pp. 484–491, 1993.

[44] D. R. Askeland and P. P. Phulé, "Mechanical properties and behavior," in *The Science and Engineering of Materials*, D. R. Askeland, Ed., 5th ed. London, U.K.: Thomson Engineering, 2006, pp. 214–215.

[45] G. Parati and L. Bernardi, "How to assess arterial compliance in humans," *J. Hypertens.*, vol. 24, no. 6, pp. 1009–1012, 2006.

[46] M. J. Roman, A. Ganau, A. P. S. Saba, R. Pini, T. G. Pickering, and R. B. Devereux, "Impact of arterial stiffening on left ventricular structure," *J. Hypertens.*, vol. 36, no. 4, pp. 489–494, 2000.

[47] J. R. Davis, "Uniaxial tensile testing," in *Tensile Testing*, J. R. Davis, Ed., 2nd ed. Novelty, OH: ASM, 2004, pp. 34–35.
[48] W. Bolton, "Stress and strain," in *Engineering Science*, W. Bolton, Ed., 5th ed. Oxford, U.K.: Elsevier, 2006, pp. 33–35.
[49] A. Ahmed and A. K. Terada, "Object detection and tracking using Kalman filter and fast mean shift algorithm," in *Proc. of VISSAPP (1)*, Feb. 5–8, 2009, pp. 585–589.
[50] B. D. Lucas and T. Kanade, "An iterative image registration technique with an application to stereo vision," in *Proc. Int. Joint Conf. Artif. Intell.*, 1981, pp. 674–679.
[51] C. Tomasi and T. Kanade, Detection and tracking of point features Carnegie Mellon Univ., Pittsburgh, PA, Tech. Rep. CMU-CS-91-132, Apr. 1991.
[52] J. Shi and C. Tomasi, "Good features to track," in *Proc. IEEE Conf. Comput. Vis. Pattern Recognit.*, 1994, pp. 593–600.
[53] G. D. Ruxon, "The unequal variance t-test is an underused alternative to student's t-test and the Mann-Whitney U test," *Behav. Ecolofy*, vol. 17, no. 4, pp. 688–690, 2006.
[54] C. W. Akerlof and F. Yuan, "Astronomical image subtraction by cross-convolution," *Astrophys. J.*, vol. 677, pp. 808–812, 2008.
[55] S. Nakaji *et al.*, "New method for the determination of fecal consistency and its optimal value in the general population," *J. Gastroenterol. Hepatol.*, vol. 17, 12, pp. 1278–1282, 2002.
[56] J. A. Ji, J. Liu, S. J. Shire, T. J. Kamerzell, S. Hong, K. Billeci, Y. Shen, and Y. J. Wang, "Characteristics of rhVEGF release from topical hydrogel formulations," *Pharm. Res.*, vol. 27, no. 4, pp. 644–654, 2010.
[57] H. H. Wenzl, K. D. Fine, L. R. Schiller, and J. S. Fordtran, "Determinants of decreased fecal consistency in patients with diarrhea," *Gastroenterology*, vol. 108, no. 6, pp. 1729–1738, 1995.
[58] D. A. Lieberman, "Clinical practice: Screening for colorectal cancer," *N. Eng. J. Med.*, vol. 361, pp. 1179–1187, 2009.
[59] S. Vijan *et al.*, "Projections of demand and capacity for colonoscopy related to increasing rates of colorectal cancer screening in the United States," *Aliment Pharmacol. Ther.*, vol. 20, no. 5, pp. 507–515, 2004.
[60] N. Schoofs, J. Devière, and A. van Gossum, "Pillcam colon capsule endoscopy compared with colonoscopy for colorectal diagnosis: A prospective pilot study," *Endoscopy*, vol. 38, no. 10, pp. 971–977, 2006.
[61] A. Van Gossum *et al.*, "Capsule endoscopy versus colonoscopy for the detection of polyps and cancer," *N. Engl. J. Med.*, vol. 361, no. 3, pp. 264–270, 2009.
[62] I. Fernandez-Urien, C. Carretero, A. Borda, and M. Munoz-Navas, "Colon capsule endoscopy," *World J. Gastroenterol.*, vol. 14, no. 34, pp. 5265–5268, 2008.
[63] C. Schmidt, "Capsule endoscopy to screen for colon cancer scores low on sensitivity, high on controversy," *JNCI J. Nat. Cancer Inst.*, vol. 101, no. 21, pp. 1444–1445, 2009.
[64] D. Filip, O. Yadid-Pecht, C. N. Andrews, and M. P. Mintchev, "Design, implementation, and testing of a miniature self-stabilizing capsule endoscope with wireless image transmission capabilities," *International J. Inf. Technol. Knowledge*, vol. 5, no. 1, pp. 3–24, 2011.
[65] J. Kannala and S. S. Brandt, "A generic camera model and calibration method for conventional, wide-angle, and fish-eye lenses," *IEEE Trans. Pattern Anal. Mach. Intell.*, vol. 28, no. 8, pp. 1335–1340, Aug. 2006.
[66] H. Wei and G. Paladini, "Image-based path planning for automated virtual colonoscopy navigation," U.S. Patent Application 0048482, Feb. 19, 2009.
[67] A. Moglia, A. Menciassi, M. O. Schurr, and P. Dario, "Wireless capsule endoscopy: From diagnostic devices to multipurpose robotic systems," *Biomed. Microdevices*, vol. 9, no. 2, pp. 235–243, 2007.
[68] J. F. Gieras, "Electric motors for medical and clinical applications," in *Advancements in Electric Machines*, J. F. Gieras, Ed. Rockford, IL: Springer, 2009, pp. 149–150.
[69] Sayaka. RF System Lab., Feb. 2011 [Online]. Available: http://www.rfamerica.com/sayaka